

Non-Parallel Voice Conversion with Augmented Classifier Star Generative Adversarial Networks

Hirokazu Kameoka, Takuhiro Kaneko, Kou Tanaka, and Nobukatsu Hojo

Abstract—We have previously proposed a method that allows for non-parallel voice conversion (VC) by using a variant of generative adversarial networks (GANs) called StarGAN. The main features of our method, called StarGAN-VC, are as follows: First, it requires no parallel utterances, transcriptions, or time alignment procedures for speech generator training. Second, it can simultaneously learn mappings across multiple domains using a single generator network so that it can fully exploit available training data collected from multiple domains to capture latent features that are common to all the domains. Third, it is able to generate converted speech signals quickly enough to allow real-time implementations and requires only several minutes of training examples to generate reasonably realistic-sounding speech. In this paper, we describe three formulations of StarGAN, including a newly introduced novel StarGAN variant called “Augmented classifier StarGAN (A-StarGAN)”, and compare them in a non-parallel VC task. We also compare them with several baseline methods.

Index Terms—Voice conversion (VC), non-parallel VC, multi-domain VC, generative adversarial networks (GANs), CycleGAN, StarGAN, A-StarGAN.

I. INTRODUCTION

Voice conversion (VC) is a task of converting the voice of a source speaker without changing the uttered sentence. Examples of the applications of VC techniques include speaker-identity modification [1], speaking assistance [2], [3], speech enhancement [4]–[6], bandwidth extension [7], and accent conversion [8].

One successful VC framework involves a Gaussian mixture model (GMM)-based approach [9]–[11], which utilizes acoustic models represented by GMMs for feature mapping. Recently, a neural network (NN)-based framework [12]–[30] and an exemplar-based framework based on non-negative matrix factorization (NMF) [31]–[33] have also proved successful. Many conventional VC methods including those mentioned above require accurately aligned parallel source and target speech data. However, in many scenarios, it is not always possible to collect parallel utterances. Even if we could collect such data, we typically need to perform time alignment procedures, which becomes relatively difficult when there is a large acoustic gap between the source and target speech. Since many frameworks are weak as regards the misalignment found with parallel data, careful pre-screening and manual correction may be required to make these frameworks work reliably. To bypass these restrictions, this paper is concerned with developing a

non-parallel VC method, which requires no parallel utterances, transcriptions, or time alignment procedures.

In general, the quality and conversion effect obtained with non-parallel methods are usually limited compared with methods using parallel data due to the disadvantage related to the training condition. Thus, developing non-parallel methods with as high a speech quality and conversion effect as parallel methods can be very challenging. Recently, some attempts have been made to develop non-parallel methods [17]–[30]. For example, a method using automatic speech recognition (ASR) was proposed in [24]. The idea is to convert input speech under the restriction that the posterior state probability of the acoustic model of an ASR system is preserved so that the transcription of the converted speech becomes consistent with that of the input speech. Since the performance of this method depends heavily on the quality of the acoustic model of ASR, it can fail to work if ASR does not function reliably. A method using i-vectors [34], known as a feature for speaker verification, was recently proposed in [25]. Conceptually, the idea is to shift the acoustic features of input speech towards target speech in the i-vector space so that the converted speech is likely to be recognized as the target speaker by a speaker recognizer. While this method is also free from parallel data, one limitation is that it is applicable only to speaker identity conversion tasks.

Recently, a framework based on conditional variational autoencoders (CVAEs) [35], [36] was proposed in [22], [29], [30]. As the name implies, variational autoencoders (VAEs) are a probabilistic counterpart of autoencoders (AEs), consisting of encoder and decoder networks. CVAEs [36] are an extended version of VAEs where the encoder and decoder networks can take a class indicator variable as an additional input. By using acoustic features as the training examples and the associated domain class labels, the networks learn how to convert source speech to a target domain according to the domain class label fed into the decoder. This CVAE-based VC approach is notable in that it is completely free from parallel data and works even with unaligned corpora. However, one well-known problem as regards VAEs is that outputs from the decoder tend to be oversmoothed. For VC applications, this can be problematic since it usually results in poor quality buzzy-sounding speech.

One powerful framework that can potentially overcome the weakness of VAEs involves generative adversarial networks (GANs) [37]. GANs offer a general framework for training a generator network so that it can generate fake data samples that can deceive a real/fake discriminator network in the form of a minimax game. While they have been found to be effective for use with image generation, in recent years they have also been

H. Kameoka, T. Kaneko, K. Tanaka, and N. Hojo are with NTT Communication Science Laboratories, Nippon Telegraph and Telephone Corporation, Atsugi, Kanagawa, 243-0198 Japan (e-mail: hirokazu.kameoka.uh@hco.ntt.co.jp).

employed with notable success for various speech processing tasks [16], [38]–[42]. We previously reported a non-parallel VC method using a GAN variant called cycle-consistent GAN (CycleGAN) [26], which was originally proposed as a method for translating images using unpaired training examples [43]–[45]. Although this method, which we call CycleGAN-VC, was shown to work reasonably well, one major limitation is that it only learns mappings between a single pair of domains. In many VC application scenarios, it is desirable to be able to convert speech into multiple domains, not just one. One naive way of applying CycleGAN to multi-domain VC tasks would be to prepare and train a different mapping pair for each domain pair. However, this can be ineffective since each mapping pair fails to use the training data of the other domains for learning, even though there must be a common set of latent features that can be shared across different domains.

To overcome the shortcomings and limitations of CVAE-VC [22] and CycleGAN-VC [26], we have previously proposed a non-parallel VC method [46] using another GAN variant called StarGAN [47], which offers the advantages of CVAE-VC and CycleGAN-VC concurrently. Unlike CycleGAN-VC and as with CVAE-VC, this method, called StarGAN-VC, is capable of simultaneously learning multiple mappings using a single generator network so that it can fully use available training data collected from multiple domains. Unlike CVAE-VC and as with CycleGAN-VC, StarGAN-VC uses an adversarial loss for generator training to encourage the generator outputs to become indistinguishable from real speech. It is also noteworthy that unlike CVAE-VC and CycleGAN-VC, StarGAN-VC does not require any information about the domain of the input speech at test time.

The remainder of this paper is organized as follows. After reviewing other related work in Section II, we briefly describe the formulation of CycleGAN-VC in Section III, present three formulations of StarGAN-VC in Section IV and show experimental results in Section V.

II. RELATED WORK

Other natural ways of overcoming the weakness of VAEs includes the VAE-GAN framework [48]. A non-parallel VC method based on this framework has already been proposed in [23]. With this approach, an adversarial loss derived using a GAN discriminator is incorporated into the training loss to encourage the decoder outputs of a CVAE to be indistinguishable from real speech features. Although the concept is similar to our StarGAN-VC approach, we will show in Section V that our approach outperforms this method in terms of both the speech quality and conversion effect.

Another related technique worth noting is the vector quantized VAE (VQ-VAE) approach [27], which has performed impressively in non-parallel VC tasks. This approach is particularly notable in that it offers a novel way of overcoming the weakness of VAEs by using the WaveNet model [49], a sample-by-sample neural signal generator, to devise both the encoder and decoder of a discrete counterpart of CVAEs. The original WaveNet model is a recursive model that makes it possible to predict the distribution of a sample conditioned on

the samples the generator has produced. While a faster version [50] has recently been proposed, it typically requires huge computational cost to generate a stream of samples, which can cause difficulties when implementing real-time systems. The model is also known to require a huge number of training examples to be able to generate natural-sounding speech. By contrast, our method is noteworthy in that it is able to generate signals quickly enough to allow real-time implementation and requires only several minutes of training examples to generate reasonably realistic-sounding speech.

Meanwhile, given the recent success of the sequence-to-sequence (S2S) learning framework in various tasks, several VC methods based on S2S models have been proposed, including the ones we proposed previously [51]–[54]. While S2S models usually require parallel corpora for training, an attempt has also been made to train an S2S model using non-parallel utterances [55]. However, it requires phoneme transcriptions as auxiliary information for model training.

III. CYCLEGAN VOICE CONVERSION

Since StarGAN-VC is an extension of CycleGAN-VC, which we also proposed previously [26], we start by briefly reviewing its formulation (Fig. 1).

Let $\mathbf{x} \in \mathbb{R}^{Q \times N}$ and $\mathbf{y} \in \mathbb{R}^{Q \times M}$ be acoustic feature sequences of speech belonging to domains X and Y , respectively, where Q is the feature dimension and N and M are the lengths of the sequences. In the following, we will restrict our attention to speaker identity conversion tasks, so when we use the term domain, we will mean speaker. The aim of CycleGAN-VC is to learn a mapping G that converts the domain of \mathbf{x} into Y and a mapping F that does the opposite. Now, we introduce discriminators D_X and D_Y , whose roles are to predict whether or not their inputs are the acoustic features of real speech belonging to X and Y , and define

$$\mathcal{L}_{\text{adv}}^{D_Y}(D_Y) = -\mathbb{E}_{\mathbf{y} \sim p_Y(\mathbf{y})}[\log D_Y(\mathbf{y})] - \mathbb{E}_{\mathbf{x} \sim p_X(\mathbf{x})}[\log(1 - D_Y(G(\mathbf{x})))] \quad (1)$$

$$\mathcal{L}_{\text{adv}}^G(G) = \mathbb{E}_{\mathbf{x} \sim p_X(\mathbf{x})}[\log(1 - D_Y(G(\mathbf{x})))] \quad (2)$$

$$\mathcal{L}_{\text{adv}}^{D_X}(D_X) = -\mathbb{E}_{\mathbf{x} \sim p_X(\mathbf{x})}[\log D_X(\mathbf{x})] - \mathbb{E}_{\mathbf{y} \sim p_Y(\mathbf{y})}[\log(1 - D_X(F(\mathbf{y})))] \quad (3)$$

$$\mathcal{L}_{\text{adv}}^F(F) = \mathbb{E}_{\mathbf{y} \sim p_Y(\mathbf{y})}[\log(1 - D_X(F(\mathbf{y})))] \quad (4)$$

as the adversarial losses for D_Y , G , D_X and F , respectively. $\mathcal{L}_{\text{adv}}^{D_Y}(D_Y)$ and $\mathcal{L}_{\text{adv}}^{D_X}(D_X)$ measure how indistinguishable $G(\mathbf{x})$ and $F(\mathbf{y})$ are from acoustic features of real speech belonging to Y and X . Since the goal of D_X and D_Y is to correctly distinguish the converted feature sequences obtained via G and F from real speech feature sequences, D_X and D_Y attempt to minimize these losses to avoid being fooled by G and F . Conversely, since one of the goals of G and F is to generate realistic-sounding speech that is indistinguishable from real speech, G and F attempt to maximize these losses or minimize $\mathcal{L}_{\text{adv}}^G(G)$ and $\mathcal{L}_{\text{adv}}^F(F)$ to fool D_Y and D_X . It can be shown that the output distributions of G and F trained in this way will match the empirical distributions $p_Y(\mathbf{y})$ and $p_X(\mathbf{x})$ if G , F , D_X , and D_Y have enough capacity [37], [43]. Note that since $\mathcal{L}_{\text{adv}}^G(G)$ and $\mathcal{L}_{\text{adv}}^F(F)$ are minimized

when $D_Y(G(\mathbf{x})) = 1$ and $D_X(F(\mathbf{y})) = 1$, we can also use $-\mathbb{E}_{\mathbf{x} \sim p_X(\mathbf{x})}[\log D_Y(G(\mathbf{x}))]$ and $-\mathbb{E}_{\mathbf{x} \sim p_X(\mathbf{x})}[\log D_Y(G(\mathbf{x}))]$ as the adversarial losses for G and F .

As mentioned above, training G and F using the adversarial losses enables mappings G and F to produce outputs identically distributed as target domains Y and X , respectively. However, using them alone does not guarantee that G or F will preserve the linguistic contents of input speech since there are infinitely many mappings that will induce the same output distributions. One way to let G and F preserve the linguistic contents of input speech would be to encourage them to make only minimal changes from the inputs. To incentivize this behaviour, we introduce a cycle consistency loss [43]–[45]

$$\mathcal{L}_{\text{cyc}}(G, F) = \mathbb{E}_{\mathbf{x} \sim p_X(\mathbf{x})}[\|F(G(\mathbf{x})) - \mathbf{x}\|_\rho^\rho] + \mathbb{E}_{\mathbf{y} \sim p_Y(\mathbf{y})}[\|G(F(\mathbf{y})) - \mathbf{y}\|_\rho^\rho], \quad (5)$$

to encourage $F(G(\mathbf{x})) \simeq \mathbf{x}$ and $G(F(\mathbf{y})) \simeq \mathbf{y}$. In image-to-image translation tasks, this regularization loss contributes to enabling G and F to change only the textures and colors of input images while preserving the domain-independent contents. However, it was non-trivial what effect this loss would have on VC tasks. Our previous work [26] was among the first to show that it enables G and F to change only the voice characteristics of input speech while preserving the linguistic content. This regularization technique has recently proved effective also in the VAE-based VC methods [56]. With the same motivation, we also consider an identity mapping loss

$$\mathcal{L}_{\text{id}}(G, F) = \mathbb{E}_{\mathbf{x} \sim p_X(\mathbf{x})}[\|F(\mathbf{x}) - \mathbf{x}\|_\rho^\rho] + \mathbb{E}_{\mathbf{y} \sim p_Y(\mathbf{y})}[\|G(\mathbf{y}) - \mathbf{y}\|_\rho^\rho], \quad (6)$$

to ensure that inputs to G and F are kept unchanged when the inputs already belong to Y and X . The full objectives of CycleGAN-VC to be minimized with respect to G , F , D_X and D_Y are thus given as

$$\mathcal{I}_{G, F}(G, F) = \lambda_{\text{adv}} \mathcal{L}_{\text{adv}}^G(G) + \lambda_{\text{adv}} \mathcal{L}_{\text{adv}}^F(F) + \lambda_{\text{cyc}} \mathcal{L}_{\text{cyc}}(G, F) + \lambda_{\text{id}} \mathcal{L}_{\text{id}}(G, F), \quad (7)$$

$$\mathcal{I}_D(D_X, D_Y) = \mathcal{L}_{\text{adv}}^{D_X}(D_X) + \mathcal{L}_{\text{adv}}^{D_Y}(D_Y), \quad (8)$$

where $\lambda_{\text{adv}} \geq 0$, $\lambda_{\text{cyc}} \geq 0$, and $\lambda_{\text{id}} \geq 0$ are regularization parameters, which weigh the importance of the adversarial, cycle consistency, and identity mapping losses. In practice, we alternately update each of G , F , D_X , and D_Y once at a time while keeping the others fixed.

IV. STARGAN VOICE CONVERSION

While CycleGAN-VC can only learn mappings between a single pair of speech domains, StarGAN-VC [46] can learn mappings among multiple speech domains using a single generator network, thus allowing us to fully utilize available training data collected from multiple domains. In this section, we describe three formulations of StarGAN. While the first and second formulations respectively correspond to the ones presented in [46] and [47], the third formulation is newly proposed in this paper with the aim of further improving the former two formulations.

A. Cross-Entropy StarGAN formulation

First, we describe the formulation we introduced in [46]. Let G be a generator that takes an acoustic feature sequence $\mathbf{x} \in \mathbb{R}^{Q \times N}$ belonging to an arbitrary domain and a target domain class index $k \in \{1, \dots, K\}$ as the inputs and generates an acoustic feature sequence $\hat{\mathbf{y}} = G(\mathbf{x}, k)$. For example, if we consider speaker identities as the domain classes, each k will be associated with a different speaker. One of the goals of StarGAN-VC is to make $\hat{\mathbf{y}} = G(\mathbf{x}, k)$ as realistic as real speech features and belong to domain k . To achieve this, we introduce a real/fake discriminator D as with CycleGAN and a domain classifier C , whose role is to predict to which classes an input belongs. D is designed to produce a probability $D(\mathbf{y}, k)$ that an input \mathbf{y} is a real speech feature whereas C is designed to produce class probabilities $p_C(k|\mathbf{y})$ of \mathbf{y} .

Adversarial Loss: First, we define

$$\mathcal{L}_{\text{adv}}^D(D) = -\mathbb{E}_{k \sim p(k), \mathbf{y} \sim p_d(\mathbf{y}|k)}[\log D(\mathbf{y}, k)] - \mathbb{E}_{k \sim p(k), \mathbf{x} \sim p_d(\mathbf{x})}[\log(1 - D(G(\mathbf{x}, k), k))], \quad (9)$$

$$\mathcal{L}_{\text{adv}}^G(G) = -\mathbb{E}_{k \sim p(k), \mathbf{x} \sim p_d(\mathbf{x})}[\log D(G(\mathbf{x}, k), k)], \quad (10)$$

as adversarial losses for discriminator D and generator G , respectively, where $p(k) = \frac{1}{K}$ (a uniform categorical distribution), $\mathbf{y} \sim p_d(\mathbf{y}|k)$ denotes a training example of an acoustic feature sequence of real speech in domain k , and $\mathbf{x} \sim p_d(\mathbf{x})$ denotes that in an arbitrary domain. $\mathcal{L}_{\text{adv}}^D(D)$ takes a small value when D correctly classifies $G(\mathbf{x}, k)$ and \mathbf{y} as fake and real speech features whereas $\mathcal{L}_{\text{adv}}^G(G)$ takes a small value when G successfully deceives D so that $G(\mathbf{x}, k)$ is misclassified as real speech features by D . Thus, we would like to minimize $\mathcal{L}_{\text{adv}}^D(D)$ with respect to D and minimize $\mathcal{L}_{\text{adv}}^G(G)$ with respect to G . Note that $\mathbb{E}_{k \sim p(k)}[\cdot]$ is a simplified notation for $\frac{1}{K} \sum_{k=1}^K (\cdot)$, and when k denotes a speaker index, $\mathbb{E}_{\mathbf{y} \sim p_d(\mathbf{y}|k)}[\cdot]$ and $\mathbb{E}_{\mathbf{x} \sim p_d(\mathbf{x})}[\cdot]$ denote the sample means over the training examples of speaker k and all speakers, respectively.

Domain Classification Loss: Next, we define

$$\mathcal{L}_{\text{cls}}^C(C) = -\mathbb{E}_{k \sim p(k), \mathbf{y} \sim p_d(\mathbf{y}|k)}[\log p_C(k|\mathbf{y})], \quad (11)$$

$$\mathcal{L}_{\text{cls}}^G(G) = -\mathbb{E}_{k \sim p(k), \mathbf{x} \sim p(\mathbf{x})}[\log p_C(k|G(\mathbf{x}, k))], \quad (12)$$

as domain classification losses for classifier C and generator G . $\mathcal{L}_{\text{cls}}^C(C)$ and $\mathcal{L}_{\text{cls}}^G(G)$ take small values when C correctly classifies $\mathbf{y} \sim p_d(\mathbf{y}|k)$ and $G(\mathbf{x}, k)$ as belonging to domain k . Thus, we would like to minimize $\mathcal{L}_{\text{cls}}^C(C)$ with respect to C and $\mathcal{L}_{\text{cls}}^G(G)$ with respect to G .

Cycle Consistency Loss: Training G , D and C using only the losses presented above does not guarantee that G will preserve the linguistic content of input speech. As with CycleGAN-VC, we introduce a cycle consistency loss to be minimized

$$\mathcal{L}_{\text{cyc}}(G) = \mathbb{E}_{k \sim p(k), k' \sim p(k), \mathbf{x} \sim p_d(\mathbf{x}|k')}[\|G(G(\mathbf{x}, k), k') - \mathbf{x}\|_\rho^\rho], \quad (13)$$

to encourage $G(\mathbf{x}, k)$ to preserve the linguistic content of \mathbf{x} , where $\mathbf{x} \sim p_d(\mathbf{x}|k')$ denotes a training example of real speech feature sequences in domain k' and ρ is a positive constant. We also consider an identity mapping loss

$$\mathcal{L}_{\text{id}}(G) = \mathbb{E}_{k' \sim p(k), \mathbf{x} \sim p_d(\mathbf{x}|k')}[\|G(\mathbf{x}, k') - \mathbf{x}\|_\rho^\rho], \quad (14)$$

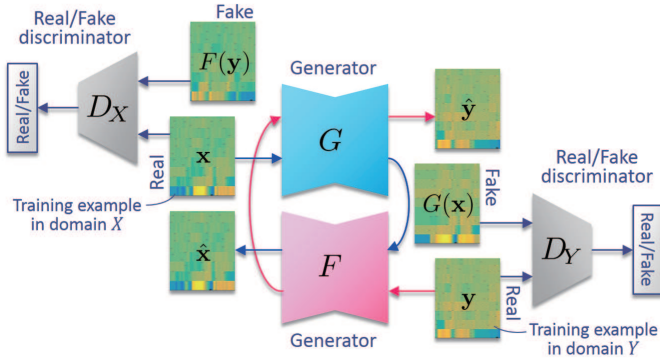


Fig. 1. Illustration of CycleGAN training.

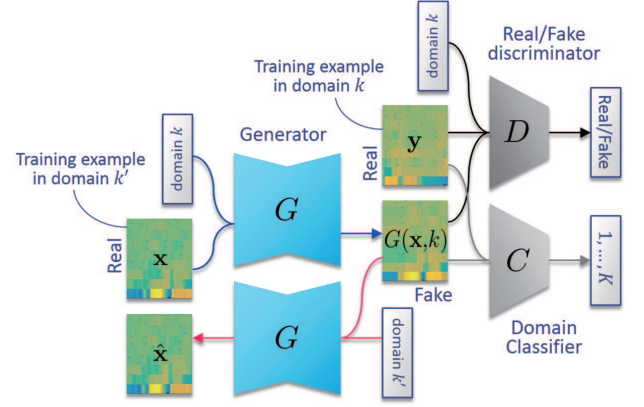


Fig. 2. Illustration of C-StarGAN training. The D network is designed to take the domain index k as an additional input and produce the probability of \mathbf{x} being a real data sample in domain k .

to ensure that an input into G will remain unchanged when the input already belongs to domain k' .

To summarize, the full objectives to be minimized with respect to G , D and C are given as

$$\mathcal{I}_G(G) = \lambda_{\text{adv}} \mathcal{L}_{\text{adv}}^G(G) + \lambda_{\text{cls}} \mathcal{L}_{\text{cls}}^G(G) + \lambda_{\text{cyc}} \mathcal{L}_{\text{cyc}}(G) + \lambda_{\text{id}} \mathcal{L}_{\text{id}}(G), \quad (15)$$

$$\mathcal{I}_D(D) = \lambda_{\text{adv}} \mathcal{L}_{\text{adv}}^D(D), \quad (16)$$

$$\mathcal{I}_C(C) = \lambda_{\text{cls}} \mathcal{L}_{\text{cls}}^C(C), \quad (17)$$

respectively, where $\lambda_{\text{adv}} \geq 0$, $\lambda_{\text{cls}} \geq 0$, $\lambda_{\text{cyc}} \geq 0$ and $\lambda_{\text{id}} \geq 0$ are regularization parameters, which weigh the importance of the adversarial, domain classification, cycle consistency, and identity mapping losses. Since the adversarial and domain classification losses in Eqs. (9), (10), (11) and (12) are defined using cross-entropy measures, we refer to this version of StarGAN as ‘‘C-StarGAN’’ (Fig. 2).

B. Wasserstein StarGAN formulation

Next, we describe the original StarGAN formulation [47]. It is frequently reported that optimization in regular GAN training can often get unstable. It has been shown that using a cross-entropy measure as the minimax objective corresponds to optimizing the Jensen-Shannon (JS) divergence between the real data distribution and the generator’s distribution [37]. As discussed in [57], the reason why regular GAN training tends to easily get unstable can be explained by the fact that the JS divergence will be maxed out when the two distributions are distant from each other so that they have disjoint supports. It is probable that this can also happen in the StarGAN training when using a cross-entropy measure. With the aim of stabilizing training, the original StarGAN adopts the Wasserstein distance, which provides a meaningful distance metric between two distributions even for those of disjoint supports, instead of the cross-entropy measure as the training objective. By using the Kantorovich-Rubinstein duality theorem [58], a tractable form of the Wasserstein distance between the real speech feature distribution $p(\mathbf{x})$ and

the distribution of the fake samples generated by the generator $G(\mathbf{x}, k)$ where $\mathbf{x} \sim p_d(\mathbf{x})$ and $k \sim p(k)$ is given by

$$\mathcal{W}(G) = \max_{D \in \mathcal{D}} \{ \mathbb{E}_{\mathbf{y} \sim p_d(\mathbf{y})} [D(\mathbf{y})] - \mathbb{E}_{k \sim p(k), \mathbf{x} \sim p_d(\mathbf{x})} [D(G(\mathbf{x}, k))] \}, \quad (18)$$

where D must lie within the space \mathcal{D} of 1-Lipschitz functions. A 1-Lipschitz function is a differentiable function that has gradients with norm at most 1 everywhere. This Lipschitz constraint is derived as a result of obtaining the above form of the Wasserstein distance [58]. As (18) shows, the computation of the Wasserstein distance requires optimization with respect to a function D . Thus, if we describe D using a neural network, the problem of minimizing $\mathcal{W}(G)$ with respect to G leads to a minimax game played by G and D similar to the regular GAN training, where D plays a similar role to the discriminator. Now, recall that the function D must be 1-Lipschitz. Although there are several ways to constrain D , such as the weight clipping technique adopted in [57], one successful and convenient way involves imposing a penalty on the sampled gradients of D

$$\mathcal{R}(D) = \mathbb{E}_{\hat{\mathbf{x}} \sim p(\hat{\mathbf{x}})} [(\|\nabla D(\hat{\mathbf{x}})\|_2 - 1)^2], \quad (19)$$

and including it in the training objective [59], where ∇ denotes the gradient operator and $\hat{\mathbf{x}}$ is a sample uniformly drawn along a straight line between a pair of a real and a generated samples. We must also consider incorporating the domain classification loss to encourage $G(\mathbf{x}, k)$ to belong to class k and the cycle-consistency loss to encourage $G(\mathbf{x}, k)$ to preserve the linguistic information in the input \mathbf{x} . Overall, the training objectives to be minimized with respect to G , D and C become

$$\mathcal{I}_G(G) = -\lambda_{\text{adv}} \mathbb{E}_{k \sim p(k), \mathbf{x} \sim p_d(\mathbf{x})} [D(G(\mathbf{x}, k))] + \lambda_{\text{cls}} \mathcal{L}_{\text{cls}}^G(G) + \lambda_{\text{cyc}} \mathcal{L}_{\text{cyc}}(G) + \lambda_{\text{id}} \mathcal{L}_{\text{id}}(G), \quad (20)$$

$$\mathcal{I}_D(D) = \lambda_{\text{adv}} \mathbb{E}_{k \sim p(k), \mathbf{x} \sim p_d(\mathbf{x})} [D(G(\mathbf{x}, k))] - \lambda_{\text{adv}} \mathbb{E}_{\mathbf{y} \sim p_d(\mathbf{y})} [D(\mathbf{y})] + \lambda_{\text{gp}} \mathbb{E}_{\hat{\mathbf{x}} \sim p(\hat{\mathbf{x}})} [(\|\nabla D(\hat{\mathbf{x}})\|_2 - 1)^2], \quad (21)$$

$$\mathcal{I}_C(C) = \lambda_{\text{cls}} \mathcal{L}_{\text{cls}}^C(C), \quad (22)$$

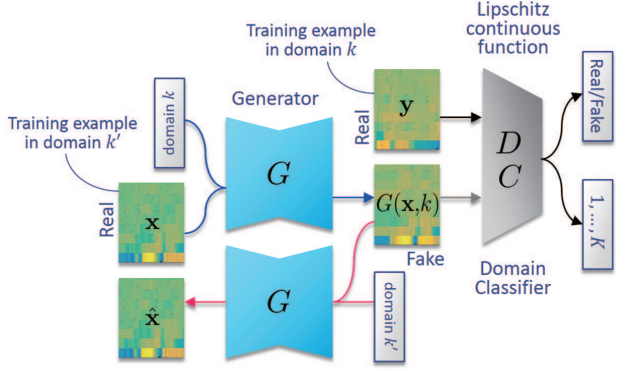


Fig. 3. Illustration of W-StarGAN training. The D and C networks are designed to share lower layers and produce the score that measures how likely \mathbf{x} is to be a real data sample and the probability of \mathbf{x} belonging to each domain.

where $\lambda_{gp} \geq 0$ is for weighing the importance of the gradient penalty. We refer to this version of StarGAN as ‘‘Wasserstein StarGAN (W-StarGAN)’’. It should be noted that the authors of [47] choose to implement D and C as a single multi-task classifier network that simultaneously produces the values $D(\mathbf{x})$ and $p_C(k|\mathbf{x})$ ($k = 1, \dots, K$) (Fig. 3).

C. Proposed New StarGAN formulation

With the two StarGAN formulations presented above, the ability of G to appropriately convert its input into a target domain depends on how the decision boundary formed by C becomes during training. The domain classification loss can be easily made almost 0 by letting the samples of $G(\mathbf{x}, k)$ resemble for example only a few of the real speech samples in domain k near the decision boundary. In such situations, G will have no incentive to attempt to make the generated samples get closer to the rest of the real speech samples distributed in domain k . As a result, the conversion effect of the trained G will be limited. One reasonable way to avoid such situations would be to consider additional classes for out-of-distribution samples that do not belong to any of the domains and encourage G to not generate samples belonging to those classes. This idea can be formulated as follows.

First, we unify the real/fake discriminator and the domain classifier into a single multiclass classifier A that outputs $2K$ probabilities $p_A(k|\mathbf{x})$ ($k = 1, \dots, 2K$) where $k = 1, \dots, K$ and $k = K + 1, \dots, 2K$ correspond to the real domain classes and the fake classes, respectively. Note that this differs from the multi-task classifier network mentioned above in that $p_A(k|\mathbf{x})$ must now satisfy $\sum_{k=1}^{2K} p_A(k|\mathbf{x}) = 1$. Here, the K fake classes can be seen as the classes for out-of-distribution samples. Next, by using this multiclass classifier, we define

$$\mathcal{L}_{adv}^A(A) = -\mathbb{E}_{k \sim p(k), \mathbf{y} \sim p_d(\mathbf{y}|k)} [\log p_A(k|\mathbf{y})] - \mathbb{E}_{k \sim p(k), \mathbf{x} \sim p_d(\mathbf{x})} [\log p_A(K+k|G(\mathbf{x}, k))], \quad (23)$$

$$\mathcal{L}_{adv}^G(G) = -\mathbb{E}_{k \sim p(k), \mathbf{x} \sim p_d(\mathbf{x})} [\log p_A(k|G(\mathbf{x}, k))] + \mathbb{E}_{k \sim p(k), \mathbf{x} \sim p_d(\mathbf{x})} [\log p_A(K+k|G(\mathbf{x}, k))], \quad (24)$$

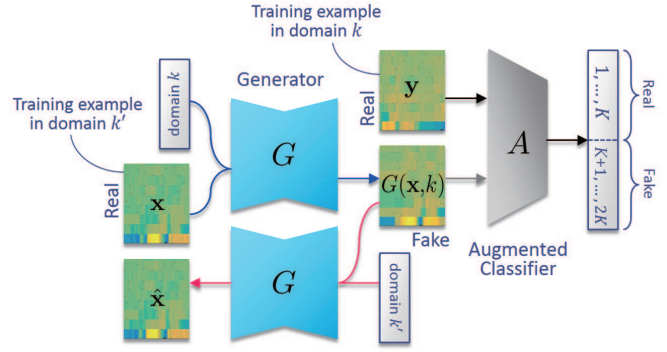


Fig. 4. Illustration of A-StarGAN training. The A network is designed to produce $2K$ probabilities, where the first and second K probabilities correspond to real and fake classes, and simultaneously play the roles of the real/fake discriminator and the domain classifier.

as adversarial losses for classifier A and generator G . $\mathcal{L}_{adv}^A(A)$ becomes small when A correctly classifies $\mathbf{y} \sim p_d(\mathbf{y}|k)$ as real speech samples in domain k and $G(\mathbf{x}, k)$ as fake samples in domain k whereas $\mathcal{L}_{adv}^G(G)$ becomes small when G fools A so that $G(\mathbf{x}, k)$ is misclassified by A as real speech samples in domain k and is not classified as fake samples.

We will show below that this minimax game reaches a global optimum when $p_d(\mathbf{y}|k) = p_G(\mathbf{y}|k)$ for $k = 1, \dots, K$ if both G and A have infinite capacity where $p_G(\mathbf{y}|k)$ denotes the distribution of $\mathbf{y} = G(\mathbf{x}, k)$ with $\mathbf{x} \sim p_d(\mathbf{x})$. We first consider the optimal classifier A for any given generator G .

Proposition 1. For fixed G , $\mathcal{L}_{adv}^A(A)$ is minimized when

$$p_A^*(k|\mathbf{y}) = \frac{p(k)p(\mathbf{y}|k)}{\sum_k p(k)p_d(\mathbf{y}|k) + \sum_k p(k)p_G(\mathbf{y}|k)}, \quad (25)$$

$$p_A^*(K+k|\mathbf{y}) = \frac{p(k)p_G(\mathbf{y}|k)}{\sum_k p(k)p_d(\mathbf{y}|k) + \sum_k p(k)p_G(\mathbf{y}|k)}, \quad (26)$$

for $k = 1, \dots, K$.

Proof: . By differentiating the Lagrangian

$$L(A, \gamma) = \mathcal{L}_{adv}^A(A) + \int \gamma(\mathbf{y}) \left(\sum_{k=1}^{2K} p_A(k|\mathbf{y}) - 1 \right) d\mathbf{y} \quad (27)$$

with respect to $p_A(k|\mathbf{y})$

$$\frac{\partial L(A, \gamma)}{\partial p_A(k|\mathbf{y})} = \begin{cases} -\frac{p(k)p_d(\mathbf{y}|k)}{p_A(k|\mathbf{y})} + \gamma(\mathbf{y}) & (1 \leq k \leq K) \\ -\frac{p(k)p_G(\mathbf{y}|k)}{p_A(k|\mathbf{y})} + \gamma(\mathbf{y}) & (K+1 \leq k \leq 2K) \end{cases}$$

and setting the result at zero, we obtain

$$p_A(k|\mathbf{y}) = \begin{cases} p(k)p_d(\mathbf{y}|k)/\gamma(\mathbf{y}) & (1 \leq k \leq K) \\ p(k)p_G(\mathbf{y}|k)/\gamma(\mathbf{y}) & (K+1 \leq k \leq 2K) \end{cases}. \quad (28)$$

Since $p_A(k|\mathbf{y})$ must sum to unity, the multiplier γ must be

$$\gamma(\mathbf{y}) = \sum_{k=1}^K p(k)p_d(\mathbf{y}|k) + \sum_{k=1}^K p(k)p_G(\mathbf{y}|k). \quad (29)$$

Substituting (29) into (28) concludes the proof. \square

Theorem 1. *The global optimum of the minimax game is achieved when $p_d(\mathbf{y}|k) = p_G(\mathbf{y}|k)$ for $k = 1, \dots, K$.*

Proof: . By substituting (25) and (26) into $\mathcal{L}_{\text{adv}}^G(G)$, we can describe it as a function of G only:

$$\begin{aligned} \mathcal{L}_{\text{adv}}^G(G) &= -\mathbb{E}_{k \sim p(k), \mathbf{y} \sim p_G(\mathbf{y}|k)} \left[\log \frac{p_A^*(k|\mathbf{y})}{p_A^*(K+k|\mathbf{y})} \right] \\ &= \mathbb{E}_{k \sim p(k), \mathbf{y} \sim p_G(\mathbf{y}|k)} \left[\log \frac{p_G(\mathbf{y}|k)}{p_d(\mathbf{y}|k)} \right] \\ &= \mathbb{E}_{k \sim p(k)} \text{KL}[p_G(\mathbf{y}|k) \| p_d(\mathbf{y}|k)], \end{aligned} \quad (30)$$

where $\text{KL}[\cdot \| \cdot]$ denotes the Kullback-Leibler (KL) divergence. Obviously, $\mathcal{L}_{\text{adv}}^G(G)$ becomes 0 if and only if $p_d(\mathbf{y}|k) = p_G(\mathbf{y}|k)$ for $k = 1, \dots, K$, thus concluding the proof. \square

We must also consider incorporating the cycle-consistency and identity mapping losses to encourage $G(\mathbf{x}, k)$ to preserve the linguistic information in the input \mathbf{x} as with the first two formulations. Overall, the training objectives to be minimized with respect to G and A become

$$\mathcal{I}_G(G) = \lambda_{\text{adv}} \mathcal{L}_{\text{adv}}^G(G) + \lambda_{\text{cyc}} \mathcal{L}_{\text{cyc}}(G) + \lambda_{\text{id}} \mathcal{L}_{\text{id}}(G), \quad (31)$$

$$\mathcal{I}_A(A) = \lambda_{\text{adv}} \mathcal{L}_{\text{adv}}^A(A). \quad (32)$$

We refer to this formulation as the ‘‘augmented multiclass classifier StarGAN (A-StarGAN)’’ (Fig. 4).

A comparative look at the C-StarGAN [46] and A-StarGAN formulations may provide intuitive insights into the behavior of the A-StarGAN training. Although not explicitly stated, with C-StarGAN, the minimax game played by G and D using (9) and (10) only is shown to correspond to minimizing the JS divergence between $p_G(\mathbf{y}|k)$ and $p_d(\mathbf{y}|k)$. While this minimax game only cares whether $G(\mathbf{x}, k)$ resembles real samples in domain k and does not concern whether $G(\mathbf{x}, k)$ is likely to belong to a different domain $k' \neq k$, A-StarGAN is designed to require $G(\mathbf{x}, k)$ to keep away from all the domains except k by explicitly penalizing $G(\mathbf{x}, k)$ for resembling real samples in domain $k' \neq k$. We expect that this particular mechanism can contribute to enhancing the conversion effect. The domain classification loss given as (12) in C-StarGAN is expected to play this role, however, its effect can be limited for the reason already mentioned. With A-StarGAN, the classifier augmented with the fake classes creates additional decision boundaries, each of which is expected to partition the region of each domain into in-distribution and out-of-distribution regions thanks to the adversarial learning and thus encourage the generator to generate samples that resemble real in-distribution samples only. It should also be noted that in C-StarGAN, when the domain classification loss comes into play, the training objective does not allow for an interpretation of the optimization process as distribution fitting, unlike A-StarGAN. This is also true for the W-StarGAN formulation.

From the above discussion, we can also think of another version of the A-StarGAN formulation, in which the K fake classes are merged into a single fake class (so the classifier A now produces only $K + 1$ probabilities) and the adversarial losses for classifier A and generator G are defined as

$$\mathcal{L}_{\text{adv}}^A(A) = -\mathbb{E}_{k \sim p(k), \mathbf{y} \sim p_d(\mathbf{y}|k)} [\log p_A(k|\mathbf{y})]$$

$$-\mathbb{E}_{k \sim p(k), \mathbf{x} \sim p_d(\mathbf{x})} [\log p_A(K+1|G(\mathbf{x}, k))], \quad (33)$$

$$\begin{aligned} \mathcal{L}_{\text{adv}}^G(G) &= -\mathbb{E}_{k \sim p(k), \mathbf{x} \sim p_d(\mathbf{x})} [\log p_A(k|G(\mathbf{x}, k))] \\ &\quad + \mathbb{E}_{k \sim p(k), \mathbf{x} \sim p_d(\mathbf{x})} [\log p_A(K+1|G(\mathbf{x}, k))]. \end{aligned} \quad (34)$$

It should be noted that the minimax game using these losses no longer leads to the minimization of the KL divergence between $p_G(\mathbf{y}|k)$ and $p_d(\mathbf{y}|k)$. However, we still believe it can work reasonably well if the augmented classifier really behaves in the way discussed above.

D. Acoustic feature

In this paper, we choose to use mel-cepstral coefficients (MCCs) computed from a spectral envelope obtained using WORLD [60], [61] as the acoustic feature to be converted. Although it would also be interesting to consider directly converting time-domain signals (for example, like [62]), given the recent significant advances in high-quality neural vocoder systems [49], [63]–[72], we would expect to generate high-quality signals by using a neural vocoder once we could obtain a sufficient set of acoustic features. Such systems can be advantageous in that the model size for the generator can be made small enough to allow the system to run in real-time and work well even when a limited amount of training data is available.

At training time, we normalize each element $x_{q,n}$ of the MCC sequence \mathbf{x} to $x_{q,n} \leftarrow (x_{q,n} - \psi_q) / \zeta_q$ where q denotes the dimension index of the MCC sequence, n denotes the frame index, and ψ_q and ζ_q denote the means and standard deviations of the q -th MCC sequence within all the voiced segments of the training samples of the same speaker.

E. Conversion process

After training G , we can convert the acoustic feature sequence \mathbf{x} of an input utterance with

$$\hat{\mathbf{y}} = G(\mathbf{x}, k), \quad (35)$$

where k denotes the target domain. Once $\hat{\mathbf{y}}$ has been obtained, we adjust the mean and variance of the generated feature sequence so that they match the pretrained mean and variance of the feature vectors of the target speaker. We can then generate a time-domain signal using the WORLD vocoder or any recently developed neural vocoder [49], [63]–[74].

F. Network architectures

The architectures of all the networks are detailed in Figs. 5–9. As detailed below, G is designed to take an acoustic feature sequence as an input and output an acoustic feature sequence of the same length so as to learn conversion rules that capture time dependencies. Similarly, D , C and A are designed to take acoustic feature sequences as inputs and generate sequences of probabilities. There are two ways to incorporate the class index k into G or D . One is to simply represent it as a one-hot vector and append it to the input of each layer. The other is to retrieve a continuous vector given k from a dictionary of embeddings and append it to each layer input, as in our previous work [52], [54]. In the following, we adopt the former way though both

performed almost the same. As detailed in Figs. 5–9, all the networks are designed using fully convolutional architectures using gated linear units (GLUs) [75]. The output of the GLU block used is defined as $\text{GLU}(\mathbf{X}) = \mathbf{X}_1 \odot \text{sigmoid}(\mathbf{X}_2)$ where \mathbf{X} is the layer input, \mathbf{X}_1 and \mathbf{X}_2 are equally sized arrays into which \mathbf{X} is split along the channel dimension, and sigmoid is a sigmoid gate function. Similar to long short-term memory units, GLUs can reduce the vanishing gradient problem for deep architectures by providing a linear path for the gradients while retaining non-linear capabilities.

Generator: As described in Figs. 5 and 6, we use a 2D CNN or a 1D CNN that takes an acoustic feature sequence \mathbf{x} as an input to design G , where \mathbf{x} is treated as an image of size $Q \times N$ with 1 channel in the 2D case or as a signal sequence of length N with Q channel in the 1D case.

Real/Fake Discriminator: We leverage the idea of PatchGANs [76] to design a real/fake discriminator or a Lipschitz continuous function D , which assigns a probability or a score to each local segment of an input feature sequence, indicating whether it is real or fake. More specifically, D takes an acoustic feature sequence \mathbf{y} as an input and produces a sequence of probabilities (with C-StarGAN) or scores (with W-StarGAN) that measures how likely each segment of \mathbf{y} is to be real speech features. With C-StarGAN, the final output of D is given by the product of all these probabilities and with W-StarGAN, the final output of D is given by the sum of all these scores.

Domain Classifier/Augmented Classifier: We also design the domain classifier C and the augmented classifier A so that each of them takes an acoustic feature sequence \mathbf{y} as an input and produces a sequence of class probability distributions that measure how likely each segment of \mathbf{y} is to belong to domain k . The final output of $p_C(k|\mathbf{y})$ or $p_A(k|\mathbf{y})$ is given by the product of all these distributions.

V. EXPERIMENTS

A. Datasets

To confirm the effects of the proposed StarGAN formulations, we conducted objective and subjective evaluation experiments involving a non-parallel speaker identity conversion task. For the experiments, we used two datasets: One is the CMU ARCTIC database [77], which consists of recordings of two female US English speakers (‘clb’ and ‘slt’) and two male US English speakers (‘bdl’ and ‘rms’) sampled at 16,000 Hz. The other is the Voice Conversion Challenge (VCC) 2018 dataset [78], which consists of recordings of six female and six male US English speakers sampled at 22,050 Hz. From the VCC2018 dataset, we selected two female speakers (‘SF1’ and ‘SF2’) and two male speakers (‘SM1’ and ‘SM2’). Thus, for each dataset, there were $K = 4$ speakers and so in total there were twelve different combinations of source and target speakers.

1) *The CMU ARCTIC Dataset:* The CMU ARCTIC dataset consisted of four speakers, each reading the same 1,132 short sentences. For each speaker, we used the first 1,000 and the latter 132 sentences for training and evaluation. To simulate a non-parallel training scenario, we divided the first 1,000

sentences equally into four groups and used only the first, second, third, and fourth groups for speakers clb, bdl, slt, and rms, so as not to use the same sentences between different speakers. The training utterances of speakers clb, bdl, slt, and rms were about 12, 11, 11, and 14 minutes long in total, respectively. For each utterance, we extracted a spectral envelope, a logarithmic fundamental frequency ($\log F_0$), and aperiodicities (APs) every 8 ms using the WORLD analyzer [60], [61]. We then extracted $Q = 28$ MCCs from each spectral envelope using the Speech Processing Toolkit (SPTK) [79].

2) *The VCC2018 Dataset:* The subset of the VCC2018 dataset consisted of four speakers, each reading the same 116 short sentences (about 7 minutes long in total). For each speaker, we used the first 81 and the latter 35 sentences (about 5 and 2 minutes long in total) for training and evaluation. Although we could actually construct a parallel corpus using this dataset, we took care not to take advantage of it to simulate a non-parallel training scenario. For each utterance, we extracted a spectral envelope, a $\log F_0$, APs, and $Q = 36$ MCCs every 5 ms using the WORLD analyzer [60], [61] and the SPTK [79] in the same manner.

For both datasets, the F_0 contours were converted using the logarithm Gaussian normalized transformation described in [80]. The APs were used directly without modification. The signals of the converted speech were obtained using the methods described in IV-E.

B. Baseline Methods

We chose the VAE-based [22] and VAEGAN-based [23] non-parallel VC methods and our previously proposed CycleGAN-VC [26] for comparison. In CycleGAN-VC, we used the same network architectures shown in Figs. 5–7 to design the generator and discriminator. To clarify how close the proposed method can get to the performance achieved by one of the best performing *parallel* VC methods, we also chose a GMM-based open-source method called ‘sprocket’ [81] for comparison. This method was used as a baseline in the VCC2018 [78]. Note that since sprocket is a parallel VC method, we tested it only on the VCC2018 dataset. To run these methods, we used the source codes provided by the authors [82]–[84].

C. Hyperparameter Settings

In the following, we use the abbreviations A-StarGAN1 and A-StarGAN2 to indicate the A-StarGAN formulations using (23) and (24) and using (33) and (34) as the adversarial losses. Hence, there were four different versions of the StarGAN formulations (namely, C-StarGAN, W-StarGAN, A-StarGAN1 and A-StarGAN2) considered for comparison.

All the networks were trained simultaneously with random initialization. Adam optimization [85] was used for model training where the mini-batch size was 16. The settings of the regularization parameters λ_{adv} , λ_{cls} , λ_{cyc} , λ_{id} , and λ_{gp} , the learning rates α_G and $\alpha_{D/C}$ for the generator and the discriminator/classifier, and the iteration number I are listed in Tab. I. For CycleGAN and all the StarGAN versions,

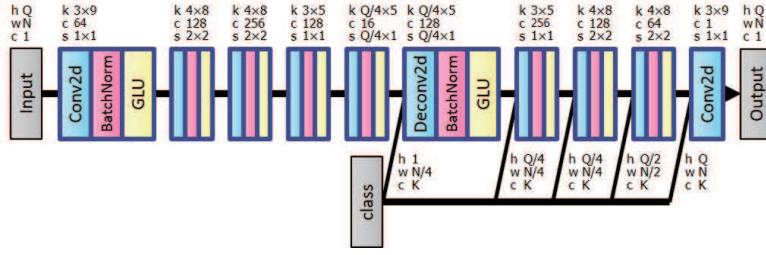


Fig. 5. Network architectures of the generator designed using 2D convolution layers. Here, the input and output of each layer are interpreted as images, where “h”, “w” and “c” denote the height, width and channel number, respectively. “Conv2d”, “BatchNorm”, “GLU”, “Deconv2d” denote 2D convolution, batch normalization, gated linear unit, and 2D transposed convolution layers, respectively. Batch normalization is applied per-channel and per-height of the input. “k”, “c” and “s” denote the kernel size, output channel number and stride size of a convolution layer, respectively. The class index, represented as a one-hot vector, is concatenated to the input of each convolution layer along the channel direction after being repeated along the height and width directions so that it has the shape compatible with the input.

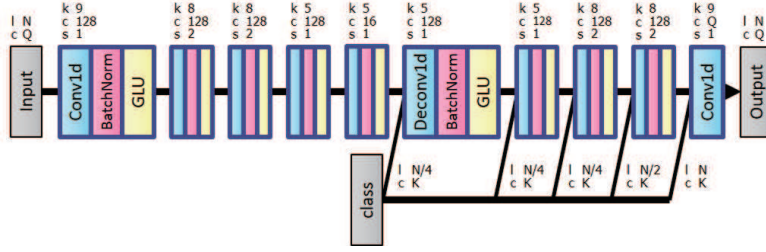


Fig. 6. Network architectures of the generator designed using 1D convolution layers. Here, the input and output of the generator are interpreted as signal sequences, where “l” and “c” denote the length and channel number, respectively. “Conv1d”, “BatchNorm”, “GLU”, “Deconv1d” denote 1D convolution, batch normalization, gated linear unit, and 1D transposed convolution layers, respectively. Batch normalization is applied per-channel of the input. The class index vector is concatenated to the input of each convolution layer after being repeated along the time direction.

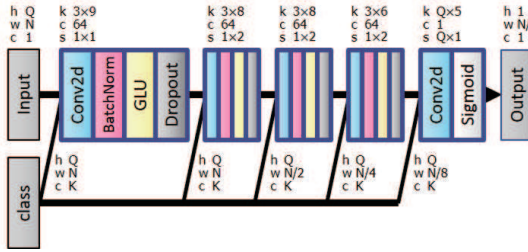


Fig. 7. Network architectures of the conditional discriminator in C-StarGAN. “Sigmoid” denotes an element-wise sigmoid function.

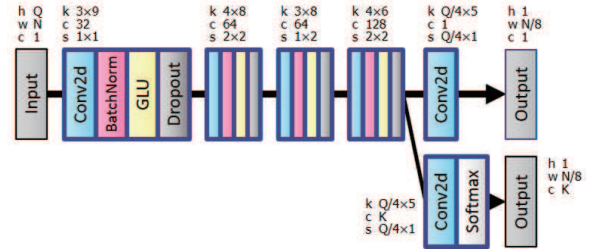


Fig. 8. Network architectures of the multi-task classifier in W-StarGAN. “Softmax” denotes a softmax function applied to the channel dimension.

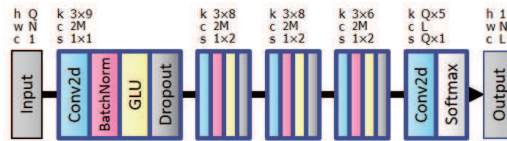


Fig. 9. Network architectures of the classifier in C-StarGAN and A-StarGAN. The output channel number L is set to K for the domain classifier in C-StarGAN, $2K$ for the augmented classifier in A-StarGAN1, and $K + 1$ for the augmented classifier in A-StarGAN2, respectively. The channel number M in the intermediate layers is set to 16 for the domain classifier in C-StarGAN and 64 for the augmented classifier in A-StarGAN1 and A-StarGAN2, respectively.

the exponential decay rate for the first moment was set at 0.9 for the generator and at 0.5 for the discriminator and classifier. Fig. 10 shows the learning curves of the four StarGAN versions under the above settings. We performed batch normalization with training mode also at test time.

D. Objective Performance Measure

In each dataset, the test set consists of speech samples of each speaker reading the same sentences. Thus, the quality of a converted feature sequence can be assessed by comparing it with the feature sequence of the target speaker reading

TABLE I
HYPERPARAMETER SETTINGS

	CycleGAN	C-StarGAN	W-StarGAN	A-StarGAN
λ_{adv}	1	1	10	1
λ_{cls}	1	1	10	1
λ_{cyc}	1	1	1	1
λ_{id}	1	1	1	1
λ_{gp}	—	—	10	—
α_G	5×10^{-4}	5×10^{-4}	5×10^{-4}	5×10^{-4}
$\alpha_{D/C}$	5×10^{-6}	2×10^{-6}	5×10^{-6}	2×10^{-6}
ρ	1	1	1	1
I	3.5×10^5	7×10^5	3.5×10^5	3.5×10^5

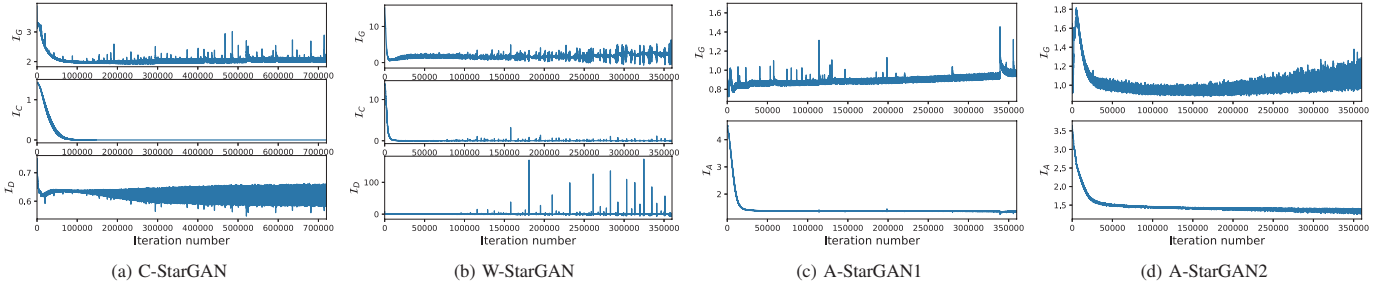


Fig. 10. Training loss curves of (a) C-StarGAN, (b) W-StarGAN, (c) A-StarGAN1, and (d) A-StarGAN2.

the same sentence. Given two mel-cepstra, $[\hat{x}_1, \dots, \hat{x}_Q]^T$ and $[x_1, \dots, x_Q]^T$, we can use the mel-cepstral distortion (MCD):

$$\text{MCD}[\text{dB}] = \frac{10}{\ln 10} \sqrt{2 \sum_{q=2}^Q (\hat{x}_q - x_q)^2}, \quad (36)$$

to measure their difference. Here, we used the average of the MCDs taken along the dynamic time warping (DTW) path between converted and target feature sequences as the objective performance measure for each test utterance.

E. Objective Evaluations

First, we evaluated the performance of each StarGAN version with different network configurations of G . The detailed settings for these configurations are shown in Figs. 5 and 6. The network architectures of the conditional discriminator and domain classifier in C-StarGAN, the multi-task classifier in W-StarGAN, and the augmented classifier in A-StarGAN are shown in Figs. 7–9. Tab. II shows the average MCDs with 95% confidence intervals obtained with these network configurations. The results show that the CycleGAN, C-StarGAN, W-StarGAN, A-StarGAN1, and A-StarGAN2 methods performed better with G designed using 1D-, 2D-, 2D-, 1D-, and 1D-CNNs, respectively. In the following, we only present the results obtained with these configurations.

Tabs. III and IV show the MCDs obtained with the proposed and baseline methods. As the results show, W-StarGAN and A-StarGAN1 performed best and next best on the CMU ARCTIC dataset, and A-StarGAN2 and A-StarGAN1 performed best and next best of all the non-parallel methods on the VCC2018 dataset. All the StarGAN versions performed consistently better than CycleGAN. Since both CycleGAN and C-StarGAN use the cross-entropy measure to define the adversarial losses, the superiority of C-StarGAN over CycleGAN reflects the effect of the many-to-many extension. Now, let us turn to the comparisons of the four StarGAN versions. From the results, we can see that W-StarGAN performed better than C-StarGAN on both datasets, revealing the advantage of the training objective defined using the Wasserstein distance with the gradient penalty. We also confirmed that A-StarGAN1&2 performed even better than W-StarGAN on the VCC2018 dataset though it performed slightly worse on the CMU ARCTIC dataset. We also confirmed that all the StarGAN versions could not yield higher performance than sprocket. Given the fact that sprocket had the advantage of using parallel data for the model training, we consider the current result to be promising, since

the proposed methods are already advantageous in that they can be applied in non-parallel training scenarios.

Balancing the learning of the palyers in a minimax game is essential in the GAN framework. The probabilities of the feature sequence converted from each test sample being real and produced by the target speaker may provide an indication of how successfully the generator, discriminator, and classifier have been trained in a balanced manner. Tabs. V and VI show the mean outputs of the discriminator and classifier of C-StarGAN, W-StarGAN, and A-StarGAN1&2 at test time. Note that since the discriminator in W-StarGAN produces scores (instead of probabilities), which are not straightforward to interpret, we have omitted them in Tab. V. As for the augmented classifier in A-StarGAN1&2, if we use $p_{k,n}$ to denote an element of the classifier output corresponding to the probability of the classifier input belonging to class k at segment n , the values $\sum_{k=1}^K p_{k,n}$ and $p_{k,n} / \sum_{k=1}^K p_{k,n}$ correspond to the probabilities of the classifier input being real and produced by speaker k , respectively, at that segment. The means of these values are shown in Tabs. V and VI. As Tabs. V and VI indicate, the generators in all the StarGAN versions were successful in confusing the discriminator and making the classifier believe that the feature sequence converted from each test sample were produced by the target speaker.

The modulation spectra of MCC sequences are known to be quantities that are closely related to perceived quality and naturalness of speech [86]. Fig. 11 shows an example of the average modulation spectra of the converted MCC sequences obtained with the proposed and baseline methods along with those of the real speech of the target speaker. As this example shows, the modulation spectra obtained with the CycleGAN-based method and all the StarGAN-based methods were relatively closer to those of real speech than the VAE-based and VAEGAN-based methods over the entire frequency range, thanks to the adversarial training strategy.

F. Subjective Listening Tests

We conducted mean opinion score (MOS) tests to compare the speech quality and speaker similarity of the converted speech samples obtained with the proposed and baseline methods. For these tests, we used the CMU ARCTIC dataset. 24 listeners (including 22 native Japanese speakers) participated in both tests. The tests were conducted online, where each participant was asked to use a headphone in a quiet environment.

TABLE II
MCD COMPARISONS OF DIFFERENT NETWORK CONFIGURATIONS OF G ON THE CMU ARCTIC DATASET

Speakers		CycleGAN		C-StarGAN		W-StarGAN		A-StarGAN1		A-StarGAN2	
src	trg	ID	2D	ID	2D	ID	2D	ID	2D	ID	2D
clb	bdl	8.34 ± .16	8.87 ± .15	7.84 ± .13	8.47 ± .14	7.72 ± .13	7.37 ± .11	7.50 ± .14	8.04 ± .15	7.57 ± .14	7.59 ± .12
	slt	7.13 ± .06	6.99 ± .06	7.45 ± .07	6.87 ± .08	7.02 ± .06	6.63 ± .05	6.56 ± .06	6.99 ± .07	6.64 ± .06	6.92 ± .06
	rms	7.64 ± .06	8.38 ± .08	8.31 ± .08	8.02 ± .08	6.87 ± .06	6.81 ± .06	7.01 ± .09	7.39 ± .08	7.23 ± .06	7.22 ± .06
bdl	clb	8.43 ± .14	8.41 ± .13	8.03 ± .12	7.75 ± .13	7.40 ± .12	7.03 ± .12	7.57 ± .13	7.80 ± .12	7.45 ± .14	7.62 ± .12
	slt	8.10 ± .11	8.29 ± .13	8.24 ± .10	8.08 ± .12	7.36 ± .10	6.85 ± .06	7.06 ± .10	7.66 ± .10	7.22 ± .09	7.27 ± .08
	rms	8.15 ± .12	8.08 ± .14	8.53 ± .12	8.09 ± .14	7.63 ± .15	7.45 ± .17	7.34 ± .16	8.09 ± .12	7.45 ± .15	7.72 ± .14
slt	clb	7.18 ± .07	7.03 ± .07	7.48 ± .09	7.04 ± .07	7.10 ± .07	6.72 ± .08	7.02 ± .08	7.12 ± .09	6.75 ± .07	7.19 ± .10
	bdl	8.48 ± .10	8.68 ± .12	7.94 ± .08	8.59 ± .12	7.79 ± .09	7.40 ± .08	7.43 ± .09	8.00 ± .10	7.53 ± .08	7.60 ± .09
	rms	8.70 ± .10	8.52 ± .08	8.67 ± .08	8.55 ± .10	7.12 ± .10	7.00 ± .09	7.26 ± .10	7.78 ± .10	7.55 ± .10	7.84 ± .13
rms	clb	7.98 ± .07	8.33 ± .10	8.04 ± .08	7.88 ± .06	7.24 ± .08	6.94 ± .07	7.23 ± .08	7.48 ± .07	7.16 ± .07	7.28 ± .07
	bdl	8.18 ± .17	8.12 ± .18	8.04 ± .18	8.49 ± .18	8.52 ± .19	8.16 ± .19	7.60 ± .19	8.33 ± .20	7.67 ± .15	7.78 ± .19
	slt	8.99 ± .09	8.67 ± .09	8.57 ± .11	8.52 ± .13	7.41 ± .10	7.11 ± .10	7.08 ± .09	7.85 ± .11	7.34 ± .11	7.55 ± .11
All pairs		8.11 ± .04	8.20 ± .04	8.09 ± .04	8.03 ± .04	7.43 ± .04	7.12 ± .04	7.22 ± .04	7.71 ± .04	7.30 ± .03	7.46 ± .03

TABLE III
MCD COMPARISONS WITH BASELINE METHODS ON THE CMU ARCTIC DATASET

Speakers		VAE	VAEGAN	CycleGAN	C-StarGAN	W-StarGAN	A-StarGAN1	A-StarGAN2
source	target							
clb	bdl	7.85 ± .10	8.82 ± .14	8.34 ± .16	8.47 ± .14	7.37 ± .11	7.50 ± .14	7.57 ± .14
	slt	7.08 ± .07	8.11 ± .06	7.13 ± .06	6.87 ± .08	6.63 ± .05	6.56 ± .06	6.64 ± .06
	rms	7.70 ± .05	8.14 ± .07	7.64 ± .06	8.02 ± .08	6.81 ± .06	7.01 ± .09	7.23 ± .06
bdl	clb	7.68 ± .09	8.86 ± .10	8.43 ± .14	7.75 ± .13	7.03 ± .12	7.57 ± .13	7.45 ± .14
	slt	7.39 ± .09	8.15 ± .08	8.10 ± .11	8.08 ± .12	6.85 ± .06	7.06 ± .10	7.22 ± .09
	rms	7.99 ± .12	8.28 ± .11	8.15 ± .12	8.09 ± .14	7.45 ± .17	7.34 ± .16	7.45 ± .15
slt	clb	6.96 ± .07	8.36 ± .09	7.18 ± .07	7.04 ± .07	6.72 ± .08	7.02 ± .08	6.75 ± .07
	bdl	7.44 ± .08	7.60 ± .09	8.48 ± .10	8.59 ± .12	7.40 ± .08	7.43 ± .09	7.53 ± .08
	rms	7.72 ± .10	8.39 ± .11	8.70 ± .10	8.55 ± .10	7.00 ± .09	7.26 ± .10	7.55 ± .10
rms	clb	7.81 ± .07	8.64 ± .09	7.98 ± .07	7.88 ± .06	6.94 ± .07	7.23 ± .08	7.16 ± .07
	bdl	8.02 ± .15	8.19 ± .17	8.18 ± .17	8.49 ± .18	8.16 ± .19	7.60 ± .19	7.67 ± .15
	slt	7.88 ± .09	8.20 ± .11	8.99 ± .09	8.52 ± .13	7.11 ± .10	7.08 ± .09	7.34 ± .11
All pairs		7.63 ± .03	8.31 ± .03	8.11 ± .04	8.03 ± .04	7.12 ± .04	7.22 ± .04	7.30 ± .03

TABLE IV
MCD COMPARISONS WITH BASELINE METHODS ON THE VCC2018 DATASET

Speakers		non-parallel methods							parallel method
source	target	VAE	VAEGAN	CycleGAN	C-StarGAN	W-StarGAN	A-StarGAN1	A-StarGAN2	sprocket
SF1	SM1	7.66 ± 0.12	7.70 ± 0.12	7.72 ± 0.13	7.52 ± 0.12	7.26 ± 0.12	7.32 ± 0.13	7.27 ± 0.13	6.91 ± 0.12
	SF2	7.53 ± 0.12	7.43 ± 0.12	7.35 ± 0.16	7.20 ± 0.14	7.16 ± 0.13	7.05 ± 0.12	6.98 ± 0.15	6.70 ± 0.13
	SM2	8.06 ± 0.14	8.04 ± 0.15	7.91 ± 0.13	7.92 ± 0.14	7.67 ± 0.12	7.69 ± 0.12	7.58 ± 0.12	7.06 ± 0.12
SM1	SF1	8.25 ± 0.10	8.20 ± 0.13	8.03 ± 0.12	7.87 ± 0.10	7.69 ± 0.10	7.58 ± 0.10	7.45 ± 0.10	7.01 ± 0.11
	SF2	7.43 ± 0.11	7.23 ± 0.12	6.95 ± 0.12	6.97 ± 0.12	6.95 ± 0.10	6.71 ± 0.12	6.66 ± 0.11	6.30 ± 0.11
	SM2	7.92 ± 0.11	7.82 ± 0.10	7.20 ± 0.09	7.32 ± 0.11	7.24 ± 0.09	7.01 ± 0.11	7.08 ± 0.10	6.58 ± 0.10
SF2	SF1	7.97 ± 0.13	7.83 ± 0.12	7.65 ± 0.13	7.59 ± 0.12	7.59 ± 0.10	7.43 ± 0.10	7.40 ± 0.11	7.21 ± 0.11
	SM1	7.38 ± 0.11	7.37 ± 0.10	7.04 ± 0.11	7.00 ± 0.11	6.91 ± 0.12	6.82 ± 0.12	6.83 ± 0.13	6.77 ± 0.11
	SM2	7.92 ± 0.12	7.78 ± 0.11	7.64 ± 0.12	7.54 ± 0.13	7.45 ± 0.12	7.49 ± 0.13	7.48 ± 0.10	6.85 ± 0.12
SM2	SF1	8.33 ± 0.15	8.20 ± 0.16	8.13 ± 0.17	8.01 ± 0.17	7.84 ± 0.15	7.75 ± 0.16	7.67 ± 0.14	7.31 ± 0.12
	SM1	7.73 ± 0.14	7.66 ± 0.14	7.20 ± 0.13	7.20 ± 0.12	7.07 ± 0.12	6.99 ± 0.13	6.97 ± 0.13	6.88 ± 0.11
	SF2	7.74 ± 0.14	7.65 ± 0.14	7.34 ± 0.16	7.25 ± 0.15	7.27 ± 0.14	7.03 ± 0.15	6.98 ± 0.15	6.78 ± 0.15
All pairs		7.83 ± 0.05	7.74 ± 0.05	7.51 ± 0.05	7.45 ± 0.05	7.35 ± 0.04	7.24 ± 0.05	7.19 ± 0.05	6.86 ± 0.04

With the speech quality test, we included the speech samples synthesized in the same way as the proposed and baseline methods (namely the WORLD synthesizer) using the acoustic features directly extracted from real speech samples. Hence, the scores of these samples are expected to show the upper limit of the performance. Speech samples were presented in random orders to eliminate bias as regards the order of the stimuli. Each listener was asked to evaluate the naturalness by selecting 5: Excellent, 4: Good, 3: Fair, 2: Poor, or 1: Bad for each utterance. The results are shown in Fig. 12. As the results show, A-StarGAN1 performed slightly better than W-

StarGAN and A-StarGAN2 (although the differences were not significant) and significantly better than C-StarGAN and the VAE and VAEGAN methods. However, it also became clear that the speech quality obtained with all the methods tested here was still perceptually distinguishable from real speech samples.

With the speaker similarity test, each listener was given a converted speech sample and a real speech sample of the corresponding target speaker and was asked to evaluate how likely they are to be produced by the same speaker by selecting 5: Definitely, 4: Likely, 3: Fair, 2: Not very likely, or 1:

TABLE V
REAL/FAKE DISCRIMINATION ACCURACY (%)

Speakers		C-StarGAN	A-StarGAN1	A-StarGAN2
source	target			
clb	bdl	63.19	48.10	41.80
	slt	76.56	47.42	28.43
	rms	16.36	51.51	40.43
bdl	clb	17.73	46.77	20.49
	slt	87.83	47.64	29.46
	rms	3.93	51.00	38.14
slt	clb	22.56	47.82	22.37
	bdl	69.25	48.42	40.71
	rms	9.56	50.53	33.65
rms	clb	28.81	48.48	25.74
	bdl	60.52	48.60	40.41
	slt	72.18	47.53	29.19
All pairs		44.04	48.65	32.56

TABLE VI
SPEAKER CLASSIFICATION ACCURACY (%)

Speakers		C-StarGAN	W-StarGAN	A-StarGAN1	A-StarGAN2
source	target				
clb	bdl	96.07	99.99	99.83	98.58
	slt	96.29	99.70	96.92	80.19
	rms	93.29	99.97	99.97	92.34
bdl	clb	94.23	99.87	99.38	87.90
	slt	96.22	98.63	99.48	86.98
	rms	90.91	99.98	99.93	93.43
slt	clb	80.78	99.38	98.78	93.66
	bdl	96.15	99.99	99.72	93.94
	rms	92.24	99.99	99.90	90.95
rms	clb	86.04	98.55	99.42	92.81
	bdl	95.65	99.99	98.51	95.74
	slt	99.98	99.99	99.36	89.11
All pairs		93.15	99.67	99.27	91.30

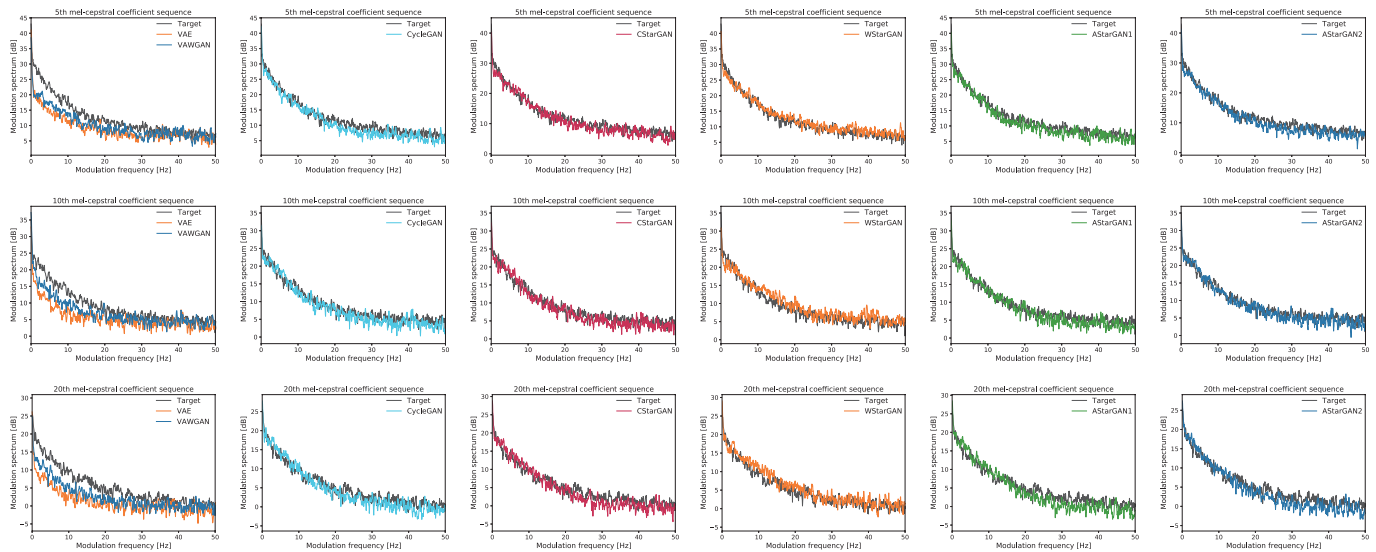


Fig. 11. Average modulation spectra of the 5-th, 10-th and 20-th dimensions of the converted MCC sequences obtained with the baseline methods and the StarGAN-based methods.

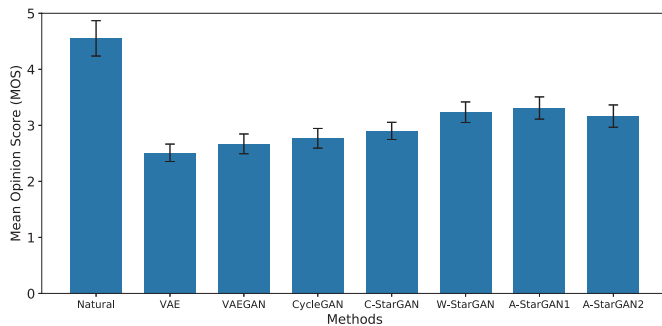


Fig. 12. Results of MOS test for speech quality

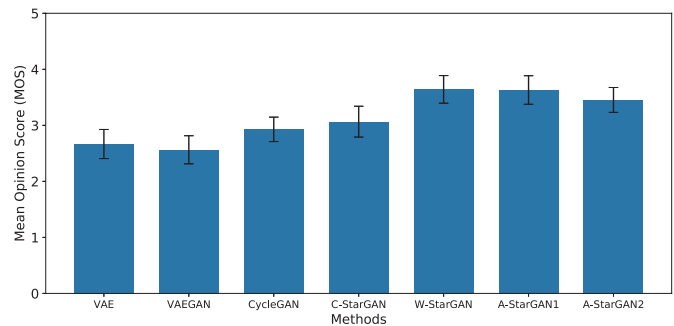


Fig. 13. Results of MOS test for speaker similarity

Unlikely. The results are shown in Fig. 13. As can be seen from the results, the W-StarGAN and A-StarGAN formulations performed comparably to each other and showed significantly better conversion ability than the remaining four methods.

VI. CONCLUSIONS

In this paper, we proposed a method that allows non-parallel multi-domain VC based on StarGAN. We described three formulations of StarGAN and compared them and several

baseline methods in a non-parallel speaker identity conversion task. Through objective evaluations, we confirmed that our method was able to convert speaker identities reasonably well using only several minutes of training examples. Interested readers are referred to [87], [88] for our investigations of other network architecture designs and improved techniques for CycleGAN-VC and StarGAN-VC.

One limitation of the proposed method is that it can only convert input speech to the voice of a speaker seen in a

given training set. It owes to the fact that one-hot encoding (or a simple embedding) used for speaker conditioning is nongeneralizable to unseen speakers. An interesting topic for future work includes developing a zero-shot VC system that can convert input speech to the voice of an unseen speaker by looking at only a few of his/her utterances. As in the recent work [89], one possible way to achieve this involves using a speaker embedding pretrained based on a metric learning framework for speaker conditioning.

ACKNOWLEDGMENT

This work was supported by JSPS KAKENHI 17H01763 and JST CREST Grant Number JPMJCR19A3, Japan.

REFERENCES

- [1] A. Kain and M. W. Macon, "Spectral voice conversion for text-to-speech synthesis," in *Proc. ICASSP*, 1998, pp. 285–288.
- [2] A. B. Kain, J.-P. Hosom, X. Niu, J. P. van Santen, M. Fried-Oken, and J. Staehely, "Improving the intelligibility of dysarthric speech," *Speech Commun.*, vol. 49, no. 9, pp. 743–759, 2007.
- [3] K. Nakamura, T. Toda, H. Saruwatari, and K. Shikano, "Speaking-aid systems using GMM-based voice conversion for electrolaryngeal speech," *Speech Commun.*, vol. 54, no. 1, pp. 134–146, 2012.
- [4] Z. Inanoglu and S. Young, "Data-driven emotion conversion in spoken English," *Speech Commun.*, vol. 51, no. 3, pp. 268–283, 2009.
- [5] O. Türk and M. Schröder, "Evaluation of expressive speech synthesis with voice conversion and copy resynthesis techniques," *IEEE Trans. ASLP*, vol. 18, no. 5, pp. 965–973, 2010.
- [6] T. Toda, M. Nakagiri, and K. Shikano, "Statistical voice conversion techniques for body-conducted unvoiced speech enhancement," *IEEE Trans. ASLP*, vol. 20, no. 9, pp. 2505–2517, 2012.
- [7] P. Jax and P. Vary, "Artificial bandwidth extension of speech signals using MMSE estimation based on a hidden Markov model," in *Proc. ICASSP*, 2003, pp. 680–683.
- [8] D. Felps, H. Bortfeld, and R. Gutierrez-Osuna, "Foreign accent conversion in computer assisted pronunciation training," *Speech Commun.*, vol. 51, no. 10, pp. 920–932, 2009.
- [9] Y. Stylianou, O. Cappé, and E. Moulines, "Continuous probabilistic transform for voice conversion," *IEEE Trans. SAP*, vol. 6, no. 2, pp. 131–142, 1998.
- [10] T. Toda, A. W. Black, and K. Tokuda, "Voice conversion based on maximum-likelihood estimation of spectral parameter trajectory," *IEEE Trans. ASLP*, vol. 15, no. 8, pp. 2222–2235, 2007.
- [11] E. Helander, T. Virtanen, J. Nurminen, and M. Gabbouj, "Voice conversion using partial least squares regression," *IEEE Trans. ASLP*, vol. 18, no. 5, pp. 912–921, 2010.
- [12] S. Desai, A. W. Black, B. Yegnanarayana, and K. Prahallad, "Spectral mapping using artificial neural networks for voice conversion," *IEEE Trans. ASLP*, vol. 18, no. 5, pp. 954–964, 2010.
- [13] S. H. Mohammadi and A. Kain, "Voice conversion using deep neural networks with speaker-independent pre-training," in *Proc. SLT*, 2014, pp. 19–23.
- [14] L. Sun, S. Kang, K. Li, and H. Meng, "Voice conversion using deep bidirectional long short-term memory based recurrent neural networks," in *Proc. ICASSP*, 2015, pp. 4869–4873.
- [15] Y. Saito, S. Takamichi, and H. Saruwatari, "Voice conversion using input-to-output highway networks," *IEICE Trans. Inf. Syst.*, vol. E100-D, no. 8, pp. 1925–1928, 2017.
- [16] T. Kaneko, H. Kameoka, K. Hiramatsu, and K. Kashino, "Sequence-to-sequence voice conversion with similarity metric learned using generative adversarial networks," in *Proc. Interspeech*, 2017, pp. 1283–1287.
- [17] L.-H. Chen, Z.-H. Ling, L.-J. Liu, and L.-R. Dai, "Voice conversion using deep neural networks with layer-wise generative training," *IEEE/ACM Trans. ASLP*, vol. 22, no. 12, pp. 1859–1872, 2014.
- [18] T. Nakashika, T. Takiguchi, and Y. Ariki, "Voice conversion based on speaker-dependent restricted Boltzmann machines," *IEICE Trans. Inf. Syst.*, vol. 97, no. 6, pp. 1403–1410, 2014.
- [19] —, "High-order sequence modeling using speaker-dependent recurrent temporal restricted Boltzmann machines for voice conversion," in *Proc. Interspeech*, 2014, pp. 2278–2282.
- [20] —, "Parallel-data-free, many-to-many voice conversion using an adaptive restricted Boltzmann machine," in *Proc. MLSP*, 2015.
- [21] M. Blaauw and J. Bonada, "Modeling and transforming speech using variational autoencoders," in *Proc. Interspeech*, 2016, pp. 1770–1774.
- [22] C.-C. Hsu, H.-T. Hwang, Y.-C. Wu, Y. Tsao, and H.-M. Wang, "Voice conversion from non-parallel corpora using variational auto-encoder," in *Proc. APSIPA*, 2016.
- [23] —, "Voice conversion from unaligned corpora using variational autoencoding Wasserstein generative adversarial networks," in *Proc. Interspeech*, 2017, pp. 3364–3368.
- [24] F.-L. Xie, F. K. Soong, and H. Li, "A KL divergence and DNN-based approach to voice conversion without parallel training sentences," in *Proc. Interspeech*, 2016, pp. 287–291.
- [25] T. Kinnunen, L. Juvela, P. Alku, and J. Yamagishi, "Non-parallel voice conversion using i-vector PLDA: Towards unifying speaker verification and transformation," in *Proc. ICASSP*, 2017, pp. 5535–5539.
- [26] T. Kaneko and H. Kameoka, "Parallel-data-free voice conversion using cycle-consistent adversarial networks," *arXiv:1711.11293 [stat.ML]*, Nov. 2017.
- [27] A. van den Oord and O. Vinyals, "Neural discrete representation learning," in *Adv. NIPS*, 2017, pp. 6309–6318.
- [28] T. Hashimoto, H. Uchida, D. Saito, and N. Minematsu, "Parallel-data-free many-to-many voice conversion based on dnn integrated with eigenspace using a non-parallel speech corpus," in *Proc. Interspeech*, 2017.
- [29] Y. Saito, Y. Ijima, K. Nishida, and S. Takamichi, "Non-parallel voice conversion using variational autoencoders conditioned by phonetic posteriorgrams and d-vectors," in *Proc. ICASSP*, 2018, pp. 5274–5278.
- [30] H. Kameoka, T. Kaneko, K. Tanaka, and N. Hojo, "ACVAE-VC: Non-parallel voice conversion with auxiliary classifier variational auto-encoder," *IEEE Trans. ASLP*, vol. 27, no. 9, pp. 1432–1443, 2019.
- [31] R. Takashima, T. Takiguchi, and Y. Ariki, "Exemplar-based voice conversion using sparse representation in noisy environments," *IEICE Trans. Inf. Syst.*, vol. E96-A, no. 10, pp. 1946–1953, 2013.
- [32] Z. Wu, T. Virtanen, E. S. Chng, and H. Li, "Exemplar-based sparse representation with residual compensation for voice conversion," *IEEE/ACM Trans. ASLP*, vol. 22, no. 10, pp. 1506–1521, 2014.
- [33] B. Sisman, M. Zhang, and H. Li, "Group sparse representation with wavenet vocoder adaptation for spectrum and prosody conversion," *IEEE/ACM Trans. ASLP*, vol. 27, no. 6, pp. 1085–1097, 2019.
- [34] N. Dehak, P. Kenny, R. Dehak, P. Dumouchel, and P. Ouellet, "Front-end factor analysis for speaker verification," *IEEE Trans. ASLP*, vol. 19, no. 4, pp. 788–798, 2011.
- [35] D. P. Kingma and M. Welling, "Auto-encoding variational Bayes," in *Proc. ICLR*, 2014.
- [36] D. P. K. D. J. Rezende, S. Mohamedy, and M. Welling, "Semi-supervised learning with deep generative models," in *Adv. NIPS*, 2014, pp. 3581–3589.
- [37] I. Goodfellow, J. Pouget-Abadie, M. Mirza, B. Xu, D. Warde-Farley, S. Ozair, A. Courville, and Y. Bengio, "Generative adversarial nets," in *Adv. NIPS*, 2014, pp. 2672–2680.
- [38] T. Kaneko, H. Kameoka, N. Hojo, Y. Ijima, K. Hiramatsu, and K. Kashino, "Generative adversarial network-based postfilter for statistical parametric speech synthesis," in *Proc. ICASSP*, 2017, pp. 4910–4914.
- [39] Y. Saito, S. Takamichi, and H. Saruwatari, "Statistical parametric speech synthesis incorporating generative adversarial networks," *IEEE/ACM Trans. ASLP*, vol. 26, no. 1, pp. 84–96, Jan. 2018.
- [40] S. Pascual, A. Bonafonte, and J. Serra, "SEGAN: Speech enhancement generative adversarial network," *arXiv:1703.09452 [cs.LG]*, Mar. 2017.
- [41] T. Kaneko, S. Takaki, H. Kameoka, and J. Yamagishi, "Generative adversarial network-based postfilter for STFT spectrograms," in *Proc. Interspeech*, 2017, pp. 3389–3393.
- [42] K. Oyamada, H. Kameoka, T. Kaneko, K. Tanaka, N. Hojo, and H. Ando, "Generative adversarial network-based approach to signal reconstruction from magnitude spectrograms," *arXiv:1804.02181 [eess.SP]*, Apr. 2018.
- [43] J.-Y. Zhu, T. Park, P. Isola, and A. A. Efros, "Unpaired image-to-image translation using cycle-consistent adversarial networks," in *Proc. ICCV*, 2017, pp. 2223–2232.
- [44] T. Kim, M. Cha, H. Kim, J. K. Lee, and J. Kim, "Learning to discover cross-domain relations with generative adversarial networks," in *Proc. ICML*, 2017, pp. 1857–1865.
- [45] Z. Yi, H. Zhang, P. Tan, and M. Gong, "DualGAN: Unsupervised dual learning for image-to-image translation," in *Proc. ICCV*, 2017, pp. 2849–2857.
- [46] H. Kameoka, T. Kaneko, K. Tanaka, and N. Hojo, "StarGAN-VC: Non-parallel many-to-many voice conversion using star generative adversarial networks," in *Proc. SLT*, 2018, pp. 266–273.

- [47] Y. Choi, M. Choi, M. Kim, J.-W. Ha, S. Kim, and J. Choo, "StarGAN: Unified generative adversarial networks for multi-domain image-to-image translation," *arXiv:1711.09020 [cs.CV]*, Nov. 2017.
- [48] A. B. L. Larsen, S. K. Sønderby, H. Larochelle, and O. Winther, "Autoencoding beyond pixels using a learned similarity metric," *arXiv:1512.09300 [cs.LG]*, Dec. 2015.
- [49] A. van den Oord, S. Dieleman, H. Zen, K. Simonyan, O. Vinyals, A. Graves, N. Kalchbrenner, A. Senior, and K. Kavukcuoglu, "WaveNet: A generative model for raw audio," *arXiv:1609.03499 [cs.SD]*, Sep. 2016.
- [50] A. van den Oord, Y. Li, I. Babuschkin, K. Simonyan, O. Vinyals, K. Kavukcuoglu, G. van den Driessche, E. Lockhart, L. C. Cobo, F. Stimberg, N. Casagrande, D. G., S. Noury, S. Dieleman, E. Elsen, N. Kalchbrenner, H. Zen, A. Graves, H. King, T. Walters, D. Belov, and D. Hassabis, "Parallel WaveNet: Fast high-fidelity speech synthesis," *arXiv:1711.10433 [cs.LG]*, Nov. 2017.
- [51] K. Tanaka, H. Kameoka, T. Kaneko, and N. Hojo, "AttS2S-VC: Sequence-to-sequence voice conversion with attention and context preservation mechanisms," in *Proc. ICASSP*, 2019, pp. 6805–6809.
- [52] H. Kameoka, K. Tanaka, D. Kwaśny, and N. Hojo, "ConvS2S-VC: Fully convolutional sequence-to-sequence voice conversion," *IEEE/ACM Trans. ASLP*, vol. 28, pp. 1849–1863, 2020.
- [53] W.-C. Huang, T. Hayashi, Y.-C. Wu, H. Kameoka, and T. Toda, "Voice transformer network: Sequence-to-sequence voice conversion using transformer with text-to-speech pretraining," *arXiv:1912.06813 [eess.AS]*, Dec. 2019.
- [54] H. Kameoka, W.-C. Huang, K. Tanaka, T. Kaneko, N. Hojo, and T. Toda, "Many-to-many voice transformer network," *arXiv:2005.08445 [eess.AS]*, 2020.
- [55] J.-X. Zhang, Z.-H. Ling, and L.-R. Dai, "Non-parallel sequence-to-sequence voice conversion with disentangled linguistic and speaker representations," *arXiv:1906.10508 [eess.AS]*, 2019.
- [56] P. L. Tobing, Y.-C. Wu, T. Hayashi, K. Kobayashi, and T. Toda, "Non-parallel voice conversion with cyclic variational autoencoder," in *Proc. Interspeech*, 2019, pp. 674–678.
- [57] M. Arjovsky and L. Bottou, "Towards principled methods for training generative adversarial networks," in *Proc. ICLR*, 2017.
- [58] C. Villani, *Optimal Transport: Old and New*, ser. Grundlehren der mathematischen Wissenschaften. Springer Berlin Heidelberg, 2008. [Online]. Available: https://books.google.co.jp/books?id=hV8o5R7_5tkC
- [59] I. Gulrajani, F. Ahmed, M. Arjovsky, V. Dumoulin, and A. Courville, "Improved training of wasserstein gans," in *Adv. NIPS*, 2017, pp. 5769–5779.
- [60] M. Morise, F. Yokomori, and K. Ozawa, "WORLD: a vocoder-based high-quality speech synthesis system for real-time applications," *IEICE Trans. Inf. Syst.*, vol. E99-D, no. 7, pp. 1877–1884, 2016.
- [61] <https://github.com/JeremyCCHsu/Python-Wrapper-for-World-Vocoder>.
- [62] J. Serrà, S. Pascual, and C. Segura, "Blow: A single-scale hyperconditioned flow for non-parallel raw-audio voice conversion," *arXiv:1906.00794 [cs.LG]*, Jun. 2019.
- [63] A. Tamamori, T. Hayashi, K. Kobayashi, K. Takeda, and T. Toda, "Speaker-dependent WaveNet vocoder," in *Proc. Interspeech*, 2017, pp. 1118–1122.
- [64] N. Kalchbrenner, E. Elsen, K. Simonyan, S. Noury, N. Casagrande, E. Lockhart, F. Stimberg, A. van den Oord, S. Dieleman, and K. Kavukcuoglu, "Efficient neural audio synthesis," *arXiv:1802.08435 [cs.SD]*, Feb. 2018.
- [65] S. Mehri, K. Kumar, I. Gulrajani, R. Kumar, S. Jain, J. Sotelo, A. Courville, and Y. Bengio, "SampleRNN: An unconditional end-to-end neural audio generation model," *arXiv:1612.07837 [cs.SD]*, Dec. 2016.
- [66] Z. Jin, A. Finkelstein, G. J. Mysore, and J. Lu, "FFNet: A real-time speaker-dependent neural vocoder," in *Proc. ICASSP*, 2018, pp. 2251–2255.
- [67] A. van den Oord, Y. Li, I. Babuschkin, K. Simonyan, O. Vinyals, K. Kavukcuoglu, G. van den Driessche, E. Lockhart, L. C. Cobo, F. Stimberg, N. Casagrande, D. Grewe, S. Noury, S. Dieleman, E. Elsen, N. Kalchbrenner, H. Zen, A. Graves, H. King, T. Walters, D. Belov, and D. Hassabis, "Parallel WaveNet: Fast high-fidelity speech synthesis," *arXiv:1711.10433 [cs.LG]*, Nov. 2017.
- [68] W. Ping, K. Peng, and J. Chen, "ClariNet: Parallel wave generation in end-to-end text-to-speech," *arXiv:1807.07281 [cs.CL]*, Feb. 2019.
- [69] R. Prenger, R. Valle, and B. Catanzaro, "WaveGlow: A flow-based generative network for speech synthesis," *arXiv:1811.00002 [cs.SD]*, Oct. 2018.
- [70] S. Kim, S. Lee, J. Song, and S. Yoon, "FloWaveNet: A generative flow for raw audio," *arXiv:1811.02155 [cs.SD]*, Nov. 2018.
- [71] X. Wang, S. Takaki, and J. Yamagishi, "Neural source-filter-based waveform model for statistical parametric speech synthesis," *arXiv:1810.11946 [eess.AS]*, Oct. 2018.
- [72] K. Tanaka, T. Kaneko, N. Hojo, and H. Kameoka, "Synthetic-to-natural speech waveform conversion using cycle-consistent adversarial networks," in *Proc. SLT*, 2018, pp. 632–639.
- [73] K. Kumar, R. Kumar, T. de Boissiere, L. Gestin, W. Z. Teoh, J. Sotelo, A. de Brebisson, Y. Bengio, and A. Courville, "MelGAN: Generative adversarial networks for conditional waveform synthesis," in *Adv. NIPS*, 2019, pp. 14910–14921.
- [74] R. Yamamoto, E. Song, and J.-M. Kim, "Parallel WaveGAN: A fast waveform generation model based on generative adversarial networks with multi-resolution spectrogram," in *Proc. ICASSP*, 2020, pp. 6199–6203.
- [75] Y. N. Dauphin, A. Fan, M. Auli, and D. Grangier, "Language modeling with gated convolutional networks," in *Proc. ICML*, 2017, pp. 933–941.
- [76] P. Isola, J.-Y. Zhu, T. Zhou, and A. A. Efros, "Image-to-image translation with conditional adversarial networks," in *Proc. CVPR*, 2017.
- [77] J. Kominek and A. W. Black, "The CMU Arctic speech databases," in *Proc. SSW*, 2004, pp. 223–224.
- [78] J. Lorenzo-Trueba, J. Yamagishi, T. Toda, D. Saito, F. Villavicencio, T. Kinnunen, and Z. Ling, "The voice conversion challenge 2018: Promoting development of parallel and nonparallel methods," *arXiv:1804.04262 [eess.AS]*, Apr. 2018.
- [79] <https://github.com/r9y9/pysptk>.
- [80] K. Liu, J. Zhang, and Y. Yan, "High quality voice conversion through phoneme-based linear mapping functions with STRAIGHT for mandarin," in *Proc. FSKD*, 2007, pp. 410–414.
- [81] K. Kobayashi and T. Toda, "sprocket: Open-source voice conversion software," in *Proc. Odyssey*, 2018, pp. 203–210.
- [82] <https://github.com/JeremyCCHsu/vae-npvc>, (Accessed on 01/25/2019).
- [83] <https://github.com/JeremyCCHsu/vae-npvc/tree/vawgan>, (Accessed on 01/25/2019).
- [84] <https://github.com/k2kobayashi/sprocket>, (Accessed on 01/28/2019).
- [85] D. Kingma and J. Ba, "Adam: A method for stochastic optimization," in *Proc. ICLR*, 2015.
- [86] S. Takamichi, T. Toda, A. W. Black, G. Neubig, S. Sakti, and S. Nakamura, "Post-filters to modify the modulation spectrum for statistical parametric speech synthesis," *IEEE/ACM Trans. ASLP*, vol. 24, no. 4, pp. 755–767, 2016.
- [87] T. Kaneko, H. Kameoka, K. Tanaka, and N. Hojo, "CycleGAN-VC2: Improved cyclegan-based non-parallel voice conversion," in *Proc. ICASSP*, 2019, pp. 6820–6824.
- [88] —, "StarGAN-VC2: Rethinking conditional methods for stargan-based voice conversion," in *Proc. Interspeech*, 2019, pp. 679–683.
- [89] K. Qian, Y. Zhang, S. Chang, X. Yang, and M. Hasegawa-Johnson, "AutoVC: Zero-shot voice style transfer with only autoencoder loss," in *Proc. International Conference on Machine Learning (ICML)*, 2019, pp. 5210–5219.